# Observations of Tropical Cyclones with a 60, 118 and 183 GHz Microwave Sounder

Shannon Brown, Bjorn Lambrigtsen, Alan Tanner,
John Oswald, Douglas Dawson and Richard Denning

Jet Propulsion Laboratory
Pasadena, CA
Shannon.T.Brown@jpl.nasa.gov

*Abstract*—**The Jet Propulsion Laboratory's High Altitude MMIC Sounding Radiometer (HAMSR) is a 25 channel microwave sounder with channels near the 60 GHz and 118 GHz oxygen lines and near the 183 GHz water vapor line. It participated in three hurricane field campaigns, CAMEX-4, TCSP and NAMMA. The absolute calibration of the HAMSR brightness temperatures is shown to be better than 1.5 K. A non-linear iterative optimal estimation based retrieval algorithm is developed to retrieve atmospheric temperature and absolute humidity profiles. Comparisons of the retrieved profiles with co-incident dropsonde profiles during NAMMA show excellent agreement at all altitudes, with the exception of a 30% residual dry bias in the absolute humidity profile above 4 km. The warm core structure of Hurricane Erin in 2001 and Hurricane Emily in 2005 is retrieved. The 60/118 GHz channels which have matched clear air weighting functions are used to assess convective intensity in the eye wall through the relative scatter darkening between the two channels.**

*Keywords-microwave sounding;tropical cyclones;warm core;eye wall;CAMEX;TCSP;NAMMA;*

## I. INTRODUCTION

The High Altitude MMIC Sounding Radiometer (HAMSR) is an atmospheric sounder which was designed and built at the Jet Propulsion Laboratory under a grant from the NASA Instrument Incubator Program in 2001 and uses the most advanced technology available to date to achieve excellent performance in a small package. HAMSR has 8 sounding channels near the 60 GHz oxygen line complex, 10 channels near the 118.75 GHz oxygen line and 7 channels near the 183.31 GHz water vapor line.

HAMSR was first deployed in the field in the 2001 Fourth Convection and Moisture Experiment (CAMEX-4) – a hurricane field campaign operating out of Jacksonville, Florida. HAMSR also participated in the Tropical Cloud Systems and Processes (TCSP) hurricane field campaign operating out of Costa Rica in 2005. In both of these campaigns, HAMSR flew as one of the payloads on the NASA high-altitude ER-2 aircraft. Most recently, HAMSR flew on the NASA DC-8 during the NASA African Monsoon Multidisciplinary Analyses (NAMMA) campaign, which took place in 2006 and operated from Cape Verde, Africa.

## II. INSTRUMENT DESCRIPTION AND CALIBRATION

### A. Instrument Description

HAMSR scans cross track below the airplane and has a $\pm$ 45° field of view. The scan system consists of two reflectors mechanically connected to a common scanning mechanism with both beams pointing along the same boresight direction. One reflector is a flat mirror for 118 and 183 GHz and the other is a parabolic mirror for 55 GHz. The size of the beam at each band is 5.7° (HPFW), and the sidelobes for all beams are well below 30 dB with a beam efficiency of >95%, providing minimal footprint contamination. The polarization of the beams rotates as the reflectors scan, with pure V-pol at nadir. The cross track sampling is done at 3° intervals and the scan period is 1.1 seconds. A table of the HAMSR frequencies and measured NEΔTs at ambient are shown in Table 1.

### B. Instrument Calibration

Each reflector scans across two calibration targets during each

TABLE I. HAMSR CHANNEL CHARACTERISITCS

| Chan # | Center freq. [GHz] | Offset [GHz] | Wt-func. Peak [mb or mm] | NEΔT [K] |
|---|---|---|---|---|
| I-1 | 118.75 | -5.500 | Sfc/[30 mm] | 0.62 |
| I-2 | " | -3.500 | Surface | 0.46 |
| I-3 | " | -2.550 | Surface | 0.68 |
| I-4 | " | -2.050 | 1000 mb | 0.92 |
| I-5 | " | -1.600 | 750 mb | 1.2 |
| I-6 | " | -1.200 | 400 mb | 0.83 |
| I-7 | " | ±0.800 | 250 mb | 0.48 |
| I-8 | " | ±0.450 | 150 mb | 0.51 |
| I-9 | " | ±0.235 | 80 mb | 0.60 |
| I-10 | " | ±0.120 | 40 mb | 0.67 |
| II-1 | 50.30 | 0 | **Sfc/[100 mm]** | 0.40 |
| II-2 | 51.76 | 0 | Surface | 0.27 |
| II-3 | 52.80 | 0 | **1000 mb** | 0.21 |
| II-4 | 53.596 | ±0.115 | **750 mb** | 0.18 |
| II-5 | 54.40 | 0 | **400 mb** | 0.17 |
| II-6 | 54.94 | 0 | **250 mb** | 0.16 |
| II-7 | 55.50 | 0 | **150 mb** | 0.17 |
| II-8 | 56.02 & 56.67 | 0 | 90 mb | 0.18 |
| III-1 | 183.31 | -17.0 | [11 mm] | 0.61 |
| III-2 | " | ±10.0 | [6.8 mm] | 0.94 |
| III-3 | " | ±7.0 | **[4.2 mm]** | 0.98 |
| III-4 | " | ±4.5 | [2.4 mm] | 1.0 |
| III-5 | " | ±3.0 | **[1.2 mm]** | 1.3 |
| III-6 | " | ±1.8 | [0.6 mm] | 1.0 |
| III-7 | " | ±1.0 | **[0.3 mm]** | 1.5 |

scan. One target is at the ambient air temperature and the other is heated to about 70°C. The reflectivity of the targets has been measured to be less than -50 dB. The temperature of each target is measured with four temperature sensors. The targets are constructed of heavy aluminum and are insulated to keep gradients across them to less that 0.25 K. The integration time on each target is about 10 times the integration time for the atmospheric measurements.

The absolute calibration of the HAMSR $T_B$s is assessed from TCSP data using the measurements taken during the accent after take-off and the descent before landing. For the channels near the absorption line, the surface will be obscured and the measured brightness temperature as a function of height will trace out a smoothed version of the temperature profile allowing one to assess gain and offset errors. During the TCSP flights, radiosondes (RaObs) were launched from the originating airport every six hours. A radiative transfer model is used, with the upper-air data from the RaObs, to model the HAMSR $T_B$s during take-off and landing. Because the land emissivity is not known exactly, only the opaque channels are compared to the model. The Rosencrantz 1998 [1] and the Liebe 1993 [2] models are used to determine the atmospheric absorption coefficient using the temperature, pressure and water vapor profiles from the RaObs. A clear atmosphere is assumed. Table 2 gives the average difference between the model and the measurements for the flights on July 5,6,9,15,16,17,23,25,27 and 28 between flight altitudes of 6 – 16 km. There is good agreement between the model and the measurements for the opaque HAMSR channels. The measurements agree to better than 1 K, with the exception of channel II-8. The uncertainty in the model comparison arises from errors in the absorption model, errors in the RaOb profiles, errors in the navigation data (altitude and attitude) and possible water condensation on the reflector cover during ascent/decent. Considering these error sources, the inherent uncertainty in the comparison can be estimated to be at approximately the 1 K level. If one assumes that potential calibration errors are common to all HAMSR channels, such as errors in the knowledge of the absolute calibration target temperature, one can infer that the absolute calibration accuracy of the channels not compared to the model (the more transparent channels) will be similar. It is conservatively estimated that the HAMSR absolute brightness temperature calibration is better than 1.5 K.

## III. GEOPHYSICAL RETRIEVAL ALGORITHM

### A. Algorithm Description

The HAMSR measurements are used to retrieve the atmospheric state. The inversion is accomplished using an iterative non-linear optimal estimator of the form [3],

$$
\begin{aligned}
\vec{x}^{(k+1)} = \vec{x}^{(k)} - \left[ S_a^{-1} + J^T S_\varepsilon^{-1} J \right]^{-1} \\
\left[ J^T S_\varepsilon^{-1} \left( \vec{T}_B - F(\vec{x}^{(k)}) \right) - S_a^{-1} \left( \vec{x}^{(k)} - \vec{x}_a \right) \right],
\end{aligned} \quad (1)
$$

TABLE II.    HAMSR COMPARISON TO MODEL

| Chan # | Avg Model – Measured Rosencrantz (1998) [K] | Std Model – Measured Rosencrantz (1998) [K] | Avg Model – Measured Liebe (1993) [K] | Std Model – Measured Liebe (1993) [K] |
|---|---|---|---|---|
| I-8 | 1.1 | 1.2 | 0.82 | 1.2 |
| I-9 | 0.83 | 1.2 | 0.26 | 1.2 |
| I-10 | 1.2 | 1.2 | 0.47 | 1.3 |
| II-5 | -0.20 | 0.75 | -0.17 | 0.74 |
| II-6 | 0.19 | 0.62 | 0.17 | 0.62 |
| II-7 | 0.03 | 0.83 | -0.01 | 0.83 |
| II-8 | -1.4 | 1.0 | -1.4 | 1.1 |
| III-5 | 0.50 | 2.4 | 0.06 | 2.4 |
| III-6 | -0.19 | 2.3 | -0.43 | 2.3 |
| III-7 | 0.20 | 2.4 | 0.13 | 2.3 |

where $\vec{x}$ is the atmospheric state vector, $\vec{T}_B$ is the 25x1 vector of HAMSR brightness temperatures, F(x) is the forward radiative transfer model and the Jacobian, J, is calculated numerically. Convergence is reached when $\left( \vec{y} - F(\vec{x}) \right)^T \left( \vec{y} - F(\vec{x}) \right) < E$, where E is an acceptable residual error. The measurement error covariance matrix, $S_\varepsilon$, is most simply represented as a diagonal matrix, with the variance of each measurement on the diagonal. The measurement error is assumed to be random additive Gaussian noise with a standard deviation equal to the NEΔT. $S_a$ is the a priori covariance matrix and represents the natural variability of the *a priori* state vector, $\vec{x}_a$.

The state vector for the retrieval takes the following form,

$$
\vec{x} = \left[ T(z_1), \ldots, T(z_N), \rho_v(z_1), \ldots, \rho_v(z_M), L(z_1), \ldots, L(z_K) \right]^T \quad (2)
$$

where T(z) is the atmospheric temperature at attitude z, $\rho_v(z)$ is the absolute humidity and L(z) is the cloud liquid water concentration. The temperature is estimated at N heights, the absolute humidity at M heights and the cloud liquid water at K heights. Currently, ice clouds are not included in the retrieval. This will degrade the retrievals in the presence of thick ice clouds containing large particles. The *a priori* information is determined using multiple realizations of the state vector derived from radiosonde profiles. The *a priori* state vector has an equivalent form as (2), where the vector components are the climatological averages of the *a priori* database. The *a priori* covariance matrix is then cov($\vec{x}_a$). The radiosonde sites selected for the database are located on islands or near the coast in the region encompassing the flight paths.

Currently a non-scattering, 1-D plane parallel radiative transfer model is used. The gaseous absorption model of [2] is used and the Rayleigh approximation is used to model the absorption by cloud liquid. A specular surface is assumed and the surface emissivity is determined from the FASTEM-2

model [4] for the ocean surface as a function of surface temperature, salinity, wind speed, frequency and incidence angle. For land, a constant emissivity is used for all channels and incidence angles. The atmosphere is divided into uniform pressure layers of thickness dp, which is currently set at 3 mb. The temperature, water vapor and cloud liquid water are estimated at discrete heights/pressure levels given by the state vector and must be linearly interpolated to the integration grid. The trapezoidal numerical integration method is used. The liquid cloud is assumed to have a base at the lifting condensation level and a top at the -15°C isotherm. The CLW profile is estimated at several levels inside of these boundaries and no liquid is assumed to be present outside of these boundaries.

## B. Algorithm Validation

The retrieved temperature and water vapor profiles are validated using dropsondes that were released from the DC-8 during the NAMMA campaign. This dataset was chosen for the validation due to the large number of dropsondes released, compared to the CAMEX-4 and TCSP campaigns. Figure 1 shows the HAMSR retrieved profiles compared to the dropsonde profiles of temperature and absolute humidity for the September 8th flight. There is excellent agreement at all altitudes between the HAMSR and the dropsonde temperature profiles. There is also good agreement for absolute humidity for altitudes less than about 4 km. There is some yet unknown systematic bias of about 30% (HAMSR drier) in the absolute humidity retrievals above 4 km.
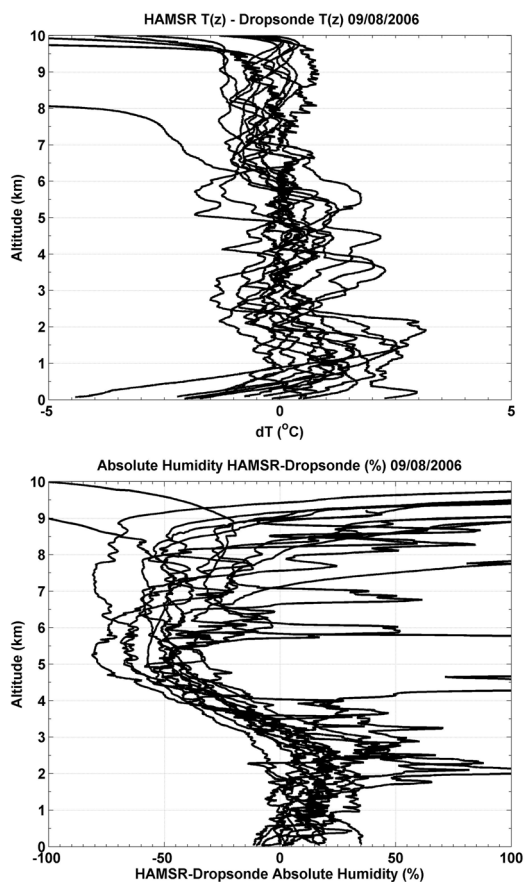
## IV. RETRIEVALS OF HURRICANE EYE STRUCTURE

### A. Warm Core Structure

The ER-2 was fortunate enough to fly over the eye of two mature hurricanes during CAMEX-4 and TCSP. The magnitude of the warm anomaly in the eye of the hurricane has been shown to be an indicator of hurricane intensity [5]. More intense storms tend to have a larger warm anomaly. The warm anomaly is found by differencing the temperature profile retrieved in the eye from an environmental profile retrieved away from the storm. Figure 2 shows the warm anomaly for Hurricane Emily on 07/17/2005 and Figure 3 shows the warm core structure for Hurricane Erin on 09/10/2001.

The maximum magnitude of the warm anomaly is similar for both hurricanes, peaking near 11-12 °C. The warmest temperatures for Hurricane Erin occur between 400-600 mb, whereas for Hurricane Emily, they occur between 150-250 mb. The inner warm core structure of Hurricane Erin derived from HASMR retrievals is very similar to the structure that was reconstructed from a dropsondes released from the ER-2 [6].

### B. Precipitation Structure

The HAMSR brightness temperature measurements can be used to indicate the convective intensity of a storm. The 60 and 118 GHz channels have nearly matched clear air weighting functions. In the presence of deep convection, the scattering depression of the brightness temperature due to the ice particle content of the cloud will be much greater at 118 GHz than at 60 GHz. Observing the difference between matched channels
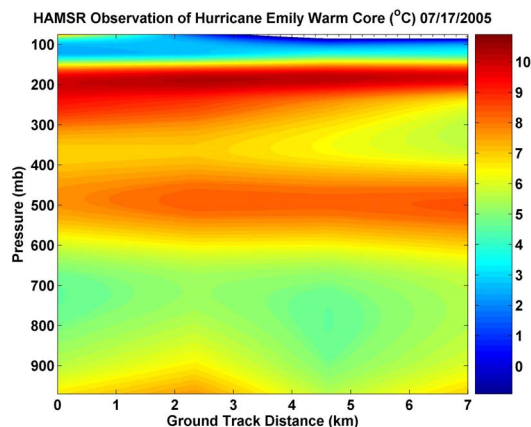


Figure 1. Comparison between HAMSR and Dropsonde temperature profiles (top) and absolute humidity profiles (bottom) for 09/08/2006.



Figure 2. Warm core structure of Hurricane Emily on 07/17/2005 derived from HAMSR.



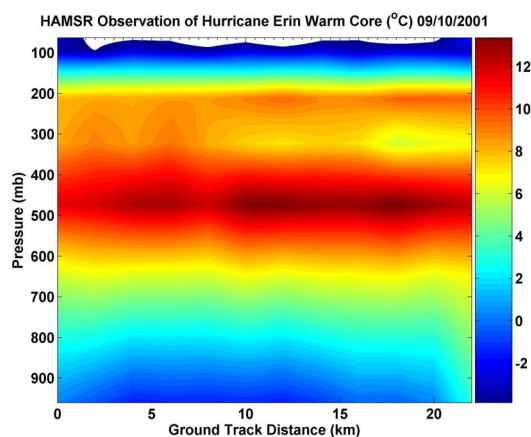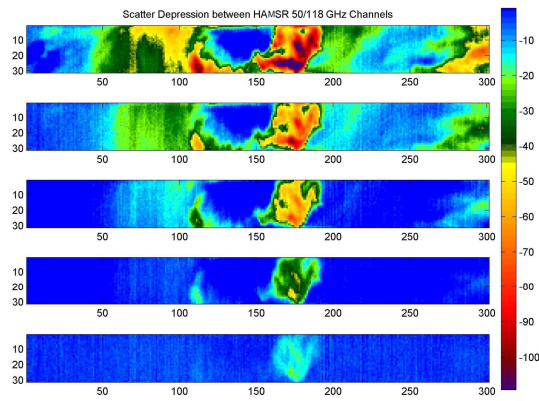Figure 3. Warm core structure of Hurrican Erin on 09/10/2001 derived from HAMSR.

Figure 4.  Relative scatter darkening between matched 60/118 GHz channels observed over Hurricane Emily on 07/17/2005.

gives an indication of both the intensity and height of the storm.  For example, the difference between channels I-7 and II-6 give an indication of ice content above about 10 km.  Figure 4 shows the precipitation structure of Hurricane Emily on 07/17/2005.  The flight path is in a north westerly direction from left to right on the image.  The top panel shows channel II-1 minus I-1.  This difference will give an indication of the intensity of the entire ice content above the melting layer.  The next panels down show the difference between II-5 and I-4, then II-6 and I-5, II-7 and I-6, II-8 and II-7, and II-9 and II-8.  It is observed that on the NW side of the eye that the convection reaches above 14 km.

## V.  CONCLUSIONS

HAMSR is a 60, 118 and 183 GHz microwave sounder which is operated by JPL.  It has flown in the CAMEX-4, TCSP and NAMMA field campaigns.  A geophysical retrieval algorithm is developed to retrieve temperature and water vapor profiles using a non-linear iterative optimal estimation based algorithm.  The retrievals are shown to have good agreement with co-incident dropsondes during NAMMA, with the exception of an unresolved 30% dry bias above 4km for the

absolute humidity profiles.  The retrieval algorithm is used to observe the warm core structure of Hurricane Erin on 09/10/2001 and Hurricane Emily on 07/17/2005.  The magnitude of the warm core is 11-12 $^{\circ}$C for both cases, but differences in the height distribution of the warm anomaly are observed.

The 60/118 GHz channels with matched clear air weighting functions are used to observe the convective intensity of Hurricane Emily.  It is shown that there is significant convection reaching to about 14 km on the NW side of the eye wall.

## REFERENCES

[1]  Rosenkranz, P.  1998.  Water Vapor Microwave Continuum Absorption: a Comparison of Measurements and Results. *Radio Science.* July-August 1998. Vol. 33. No. 4. pp. 919-28.

[2]  Liebe, H., G. A. Hufford, and M. G. Cotton.  1993.  "Propagation Modeling of Moist Air and Suspended Water Particles at Frequencies Below 1000 GHz." *Atmospheric Propagation Effects through Natural and Man-Made Obscurants for Visible to MM-Wave Radiation* (AGARD-CP-542). AGARD. Neuilly sur Seine. France. 195 pages

[3]  Rodgers, C.  2000.  Inverse Methods for Atmospheric Sounding: Theory and Practice. World Scientific. New Jersey. pp. 81-90.

[4]  Deblonde, G. and S. English.  2001.  Evaluation of the FASTEM-2 fast microwave oceanic surface emissivity model.  *Tech. Proc. ITSC-XI. Budapest.* 20-26 September 2000.  67-78.

[5]  Velden, C.  1989.  Observational Analyses of North Atlantic Tropical Cyclones from NOAA Polar-Orbiting Satellite Microwave Data. *J. Apl. Meteo.* 28. pp. 59-70.

[6]  Halverson, J.  J. Simpson, G. Heymsfield, H. Pierce, T. Hock, L. Ritchie. 2006.  Warm Core Structure of Hurricane Erin Diagnosed from High Altitude Dropsondes during CAMEX-4. *J. Atm. Sci.* 63. pp. 309-324.